Influence of incident light polarization on photonic nanojet

Yong Liu (刘 勇)[1,2], Baoyong Wang (王保勇)[1], and Zhihua Ding (丁志华)[1*]

[1]*State Key Lab of Modern Optical Instrumentation, Zhejiang University, Hangzhou 310027, China*

[2]*Department of Physics, Zhaoqing University, Zhaoqing 526061, China*

[*]*Corresponding author: zh_ding@zju.edu.cn*

Received December 15, 2010; accepted January 28, 2011; posted online May 18, 2011

Dielectric microspheres can confine light in a three-dimensional (3D) region called photonic nanojet is shown when they are illuminated by different polarized beams. The influence of incident light polarization on photonic nanojet using the finite-difference time-domain (FDTD) method is demostrated. The axial field intensity profiles of photonic nanojets for both the linear and circular polarization incident beams are very similar. Azimuthal polarization incident beam induces a doughnut beam along the optical axis, while the radial polarization incident beam permits one to reach an effective volume as small as $0.7(\lambda/n)^3$.

OCIS codes: 290.5850, 180.0180, 290.5855.

doi: 10.3788/COL201109.072901.

To obtain nanoscale information from an object by optical system, great efforts have been exerted in looking for new methods that can break through the diffraction limit or the Rayleigh limit[1,2]. In these methods, subwavelength concentration of light is often needed, and metallic structures[3−5] based on surface plasmon modes are widely used, such as tips, gratings, pinholes, and nanoparticles. Light losses in metals and challenging nanofabrication processes may limit their applications. Thus, finding a simpler optical system is necessary. When a lossless dielectric microcylinder or microsphere with a diameter larger than the wavelength is illuminated by light under certain conditions, a special nonresonant propagating beam called photonic nanojet[6−11] is created due to interferences between the illuminating field and the scattering field. Photonic nanojet has been used in laser cleaning, nanopatterning, fluorescence correlation spectroscopy, Raman spectroscopy, and optical data storage due to its properties of high intensity, subwavelength waist, and ability to propagate over a distance longer than wavelength.

Owing to its large dimension along the optical axis, the photonic nanojet often does not achieve three-dimensional (3D) subwavelength light confinement and performs no better than the focusing obtained by a classic microscope objective with a high numerical aperture (NA). According to the scattering theory of microparticle[12], when a homogeneous microparticle is illuminated by the linear or circular polarized plane wave, photonic nanojets[13−15] mainly depend on three parameters, namely, diameter of microsphere, wavelength of incident light, and the ratio of refractive index between microsphere and background. The construction of the microparticle can also change the scattering field and even affect photonic nanojet, such as the graded-index microsphere[16,17] and the two-layered microsphere[18] with different refractive indices and shell thicknesses. In fact, tight focusing is also often affected by polarization and the light field of an incident beam. Spatial inhomogeneous polarization light[19] (radial or azimuthal polarization) has drawn much attention because of its new characteristics that can create smaller focus. When the special polarized incident light is used to illuminate a microsphere, photonic nanojet may obtain very small effective volume, allowing it to be used in 3D subwavelength microscopes.

This letter investigates the light confinement produced by a dielectric microsphere illuminated by different polarization beams. Our simulations used the finite-difference time-domain (FDTD) method[20] based on the rigorous electromagnetic theory by Lumerical Solutions Inc.. We also used the configuration of a 2-μm-diameter latex sphere ($D_{\rm s}$ = 4 μm) of refractive index $n_{\rm s}$ = 1.6 surrounded by water (n = 1.33) (Fig. 1). When vacuum wavelength of the incident beam with amplitude of 1 was 633 nm, the optical parameter $\Phi = D_{\rm s}n_{\rm s}/\lambda n$ was 3.9. Linear, circular, radial, and azimuthal polarization plane-wave beams were chosen to simplify the numerical simulations and show the influence of polarization on photonic nanojet.

Figure 2 shows the electric field intensity map when the incident plane-wave beam with different polarizations is scattered by a microsphere resulting in the concentration of light and strong field intensity. The white circle in the intensity map represents the cross section of the microsphere, and the gray scales show the magnitude of field intensity. Compared with linear and circular polarizations, in the cross section along the optical axis, radial polarization shows polarization aligned in the radial direction. Similarly, azimuthal polarization shows the electric field aligned in the azimuthal direction. According to these intensity maps, the magnitude and shape of photonic nanojet both change with different polarization incident beams. The changes of the photonic nanojet demonstrate its maximum field intensity. In addition,

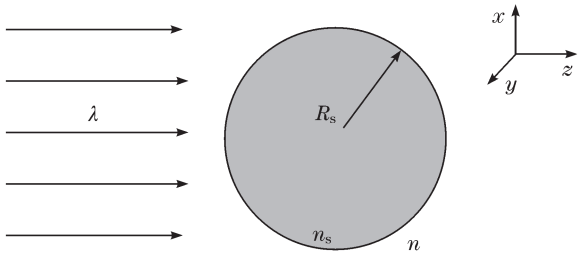

Fig. 1. Microsphere configuration for the photonic nanojet.

effective volume can be controlled by the polarization of the incident beam, except for the diameter and refractive index of the microsphere, wavelength of incident beam, and the refractive index of the background. Polarization of incident beam is a very important parameter, which is helpful in the search for longitudinally and transversally subwavelength photonic nanojets. This enables photonic nanojet to break through the diffraction limit, resulting in a broader range of applications.

The field intensity of photonic nanojet is also observed to be non-symmetric along the optical axis (Figs. 2(a) and (b)), much like a linear polarized beam tightly focused by a high NA objective. When the direction of polarization shows cylindrical symmetry, such as circular, radial, and azimuthal polarizations, this is not the case. For nanopatterning, it is necessary to pay more attention to the unsymmetric field that creates a distorted pattern. Compared with the spatial homogeneous polarization, spatial inhomogeneous polarization incident beams have numerous sidelobes on both sides of the photonic nanojet that are stronger compared with the others. In addition, the scattering field in the microsphere is mainly distributed along the margin of surface. Based on the law of conservation of energy, these strong sidelobes will decrease the maximum magnitude of field intensity (Fig. 2). Azimuthal polarization incident beam induces a doughnut beam along the optical axis. Using the generalized cylindrical vector beam makeup of radial and azimuthal polarization beams results in a subwavelength optical bubble around the light field which can be used for nanoscale optical manipulation[21].

In order to understand the change of effective volume in the photonic nanojet, the normalized field intensity along the optical axis and the transversal plane through the maximum field intensity point $I_{\max}$ are shown (Fig. 3). In this case, the longitudinal intensity distribution is apparently no more symmetric with respect to the

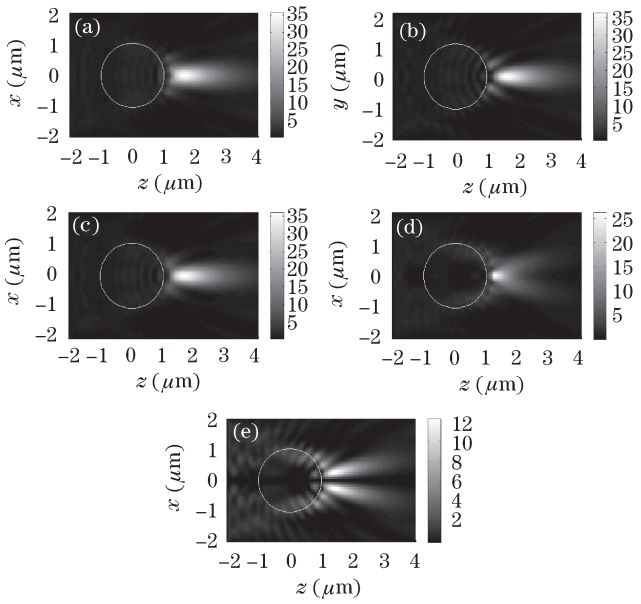

Fig. 2. Electric field intensity maps of photonic nanojets for different polarization incident beams. (a) In $x-z$ plane for x-axis linear polarization; (b) in $y-z$ plane for x-axis linear polarization; (c) circular polarization; (d) radial polarization; (e) azimuthal polarization.

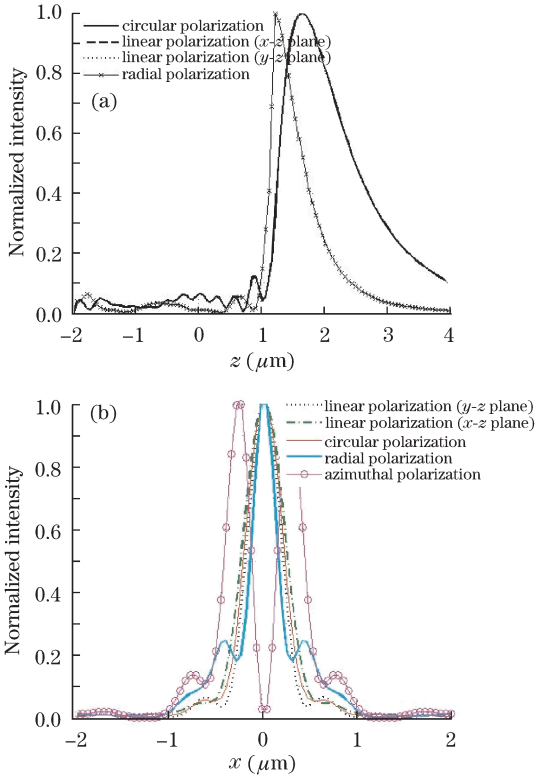

Fig. 3. Normalized electric field intensity distributions of photonic nanojet corresponding to Fig. 1. (a) Along optical axis and (b) transverse line through the maximum point of field intensity $I_{\max}$.

$I_{\max}$ position; in comparison, the transversal intensity distribution is symmetric. This is a shortcoming of the photonic nanojet, which often cannot induce the axial light confinement subwavelength level. When the microsphere is illuminated by linear and circular polarization beams, the axial field intensity profile is the same. Compared with linear and circular polarizations, both the transverse full-width at half-maximum (FWHM) and axial half-decay length in water of the photonic nanojet are clearly decreased by the radial polarization incident beam, with the maximum intensity being close to the microsphere. When the effective volume of the photonic nanojet behind the sphere is defined by $\pi^{3/2}w_{xy}^2 w_z/2$, the effective volumes are $7.9(\lambda/n)^3$ and $0.7(\lambda/n)^3$ for circular and radial polarizations, respectively, and are approximately reduced by one order of magnitude because of polarization. Taking into account the field distribution of the incident beam[22] as well as the construction of the microsphere, the photonic nanojet may be compressed further. It must be stressed that the radial polarization incident beam can effectively make a photonic nanojet a 3D subwavelength, increasing its potential for applications in 3D microscopes.

In conclusion, we demonstrate that the shape and magnitude of photonic nanojet that emerge from a microsphere can also be changed by the polarization of incident beam. When microsphere is illuminated by linear and circular polarization beams, the axial field intensity profiles are same. Azimuthal polarization incident beam creates a doughnut beam along the optical axis. The 3D subwavelength-level volume of photonic nanojet is

observed, particularly when illuminating a microsphere with a radial polarization incident beam. The design of the photonic nanojet must be based on the following parameters: diameter and construction of microsphere, wavelength, polarization and field distribution of incidence beam, and ratio of refractive index between the microsphere and background. These enable light 3D subwavelength to be confined, thus allowing the use of the photonic nanojet in more applications.

This work was supported by the National Natural Sciences Foundation of China under Grant Nos. 60978037 and 60878057.

References

1. Z. Mao, C. Wang, and Y. Cheng, Chinese J. Laser (in Chinese) **35,** 1283 (2008).
2. C. Guo, W. Ye, X. Yuan, J. Zhang, C. Zeng, and J. Ji, Acta Opt. Sin. (in Chinese) **29,** 3272 (2009).
3. J. C. Weeber, A. Bouhelier, G. C. des Francs, L. Markey, and A. Dereux, Nano Lett. **7,** 1352 (2007).
4. S. Nie and S. R. Emory, Science **275,** 1102 (1997).
5. A. Sentenac and P. C. Chaumet, Phys. Rev. Lett. **101,** 013901 (2008).
6. Z. Chen, A. Taflove, and V. Backman, Opt. Express **12,** 1214 (2004).
7. M. Mosbacher, H.-J. Münzer, J. Zimmermann, J. Solis, J. Boneberg, and P. Leiderer, Appl. Phys. A: Mater. Sci. Process. **72,** 41 (2001).
8. K. Piglmayer, R. Denk, and D. Bauerle, Appl. Phys. Lett. **80,** 4693 (2002).
9. E. McLeod and C. B. Arnold, Nature Nanotechnol. **3,** 413 (2008).
10. D. Gérard, J. Wenger, A. Devilez, D. Gachet, B. Stout, N. Bonod, E. Popov, and H. Rigneault, Opt. Express **16,** 15297 (2008).
11. S. C. Kong, A. Sahakian, A. Taflove, and V. Backman, Opt. Express **16,** 13713 (2008).
12. M. Born and E. Wolf, *Principles of Optics* (Phei, Beijing, 2006) p. 634.
13. S. Lecler, Y. Takakura, and P. Meyrueis, Opt. Lett. **30,** 2641 (2005).
14. P. Ferrand, J. Wenger, A. Devilez, M. Pianta, B. Stout, N. Bonod, E. Popov, and H. Rigneault, Opt. Express **16,** 6930(2008).
15. H. Ding, L. Dai, and C. Yan, Chin. Opt. Lett. **8,** 706 (2010).
16. S. C. Kong, A. Taflove, and V. Backman, Opt. Express **17,** 3722 (2009).
17. C. M. Ruiz and J. J. Simpson, Opt. Express **18,** 16805 (2010).
18. Y. E. Geints, E. K. Panina, and A. A. Zemlyanov, Opt. Commun. **283,** 4775 (2010).
19. Q. Zhan, Adv. Opt. Photon. **1,** 1 (2009).
20. A.Taflove and S. C. Hagness, *Computational Electrodynamics: the Finite-Difference Time-Domain Method* (Artech, Boston, 2005).
21. X. Cui, D. Erni, and C. Hafner, Opt. Express **16,** 13560 (2008).
22. A. Devilez, N. Bonod, J. Wenger, D. Gérard, B. Stout, H. Rigneault, and E. Popov, Opt. Express **17,** 2089 (2009).